Mon. Not. R. Astron. Soc. **373,** 449–456 (2006) doi:10.1111/j.1365-2966.2006.11070.x

Space very long baseline interferometry observations of polarization in the jet of 3C 380

A. Papageorgiou,[1,2⋆] T. V. Cawthorne,[1] A. Stirling,[1,3] D. Gabuzda[4] and A. G. Polatidis[5]

[1]*University of Central Lancashire, Preston PR1 2HE*
[2]*Cork Institute of Technology, Rossa Avenue, Bishopstown, Cork*
[3]*University of Manchester, Jodrell Bank Observatory, Macclesfield, Cheshire SK11 9DL*
[4]*University College Cork, Cork*
[5]*Max Planck Institut für Radioastronomie, Postfach 2024, D-53010, Bonn, Germany*

Accepted 2006 September 13. Received 2006 September 12; in original form 2006 August 2

ABSTRACT

A comparison between low-frequency space very long baseline interferometry (VLBI) and high-frequency ground-based VLBI images can, in principle, be used to detect small variations in rotation measure (RM) on fine angular scales inaccessible to ground arrays alone. This paper reports an attempt to perform such a comparison using the jet in the quasar 3C 380. Observations made with the VSOP antenna *HALCA* together with a ground array at wavelength 1.6 GHz provide total intensity and polarization images of comparable resolution to those from the ground array alone at 5 GHz. The results provide an image showing derotated magnetic vector position angle of somewhat higher resolution than that available earlier. The results show variations in an RM around component A of the order of 10 rad m^{-2} that could not have been detected with the ground array alone. It is concluded that satellite VLBI observations provide a promising means to study the distribution of matter and magnetic fields around parsec-scale jets.

The ground observations used here follow the steady outward drift of component A, which has approximately doubled its distance from the core since the first observations in 1982. They also reveal total intensity and polarization structure associated with a bright knot 0.7 arcsec from the core which is reminiscent of that expected for a conical shock wave.

Key words: galaxies: active – galaxies: jets – quasars: individual: 3C 380 (1828+487).

1 INTRODUCTION

Mapping the rotation measure (RM) provides the only possible means to study the distribution of gas and magnetic fields in the immediate environment of parsec-scale jets. Near the core region, where the high-frequency polarization is often very bright and the RMs are large, such mapping is easily performed using very long baseline interferometry (VLBI) ground arrays, such as the Very Long Baseline Array. Farther from the core, where RMs are much smaller, such measurements often prove impossible with ground arrays alone since, at high frequencies where the jet is well resolved, the RMs are sufficiently small that differences between polarization angles at neighbouring frequencies cannot easily be measured. For example, RM variations of the order of 10 rad m^{-2} correspond to EVPA differences of only a few degrees between frequencies 5 and 15 GHz, and are therefore very difficult to detect using observations at these wavelengths. Between frequencies 1.6 and 5 GHz, however, an RM variation of 10 rad m^{-2} corresponds to a difference of over 15°, and should be detectable in well-calibrated observations. However, if such variations occur over scales of an order of a few mas, baselines longer than those of ground-based VLBI arrays are needed if they are to be resolved.

This paper reports an attempt to map such RM variation in the quasar 3C 380, which has been extensively studied in total intensity on mas scales by Polatidis & Wilkinson (1998). It is classified as a compact, steep-spectrum (CSS) source having spectral index $\alpha = -0.7$. On kpc scales, 3C 380 appears as a one-sided jet with two bright knots, observed both in radio and in optical, embedded in a diffuse halo (Wilkinson et al. 1991; O'Dea et al. 1999). On parsec-scales, 3C 380 displays a twisted one-sided radio jet with a sharp apparent bend and components with superluminal motion, whose kinematic properties have been monitored for the past 20 yr (Polatidis & Wilkinson 1998). Polarization VLBI images of 3C 380 have been published by Cawthorne et al. (1993) and Taylor (1998). The first RM mapping of this source was reported by Taylor (1998)

⋆E-mail: apapageorgiou@cit.ie

using ground-based VLBI at frequencies 5 GHz and higher. This work revealed very high RMs of several thousand rad m^{-2} near the core, and lower RMs in the region of component A and beyond. It is in these regions remote from the core that small variations in RM, to which Taylor's observations would have been insensitive, are sought in the work presented here.

Two further aspects of the source are also discussed, using the ground-based observations alone. The first is component A, which stands out as a bright knot of emission, easily distinguishable in an otherwise continuous jet. The component is now approximately 9 mas north-west from the core and has been found to move superluminally at a direction of -30° (Polatidis & Wilkinson 1998) and is associated with an apparent sharp bend in the jet's direction. Polarization observations of 3C 380 by Cawthorne et al. (1993) reveal that the EVPA at component A is rotated relative to that farther down the jet, while multifrequency observations by Taylor (1998) provide a value for the magnetic vector position angle (MVPA) of $-84^\circ \pm 4^\circ$. The fractional polarization of component A increased from $\sim$4 to $\sim$12 per cent between these two epochs.

Secondly, we consider two knots of emission located at approximately 0.73 and 1 arcsec north-west from the core (hereafter referred to as K1 and K2, respectively). Although there is no observable radio emission connecting the knots with the parsec-scale jet, the fact that they both lie approximately in the direction of the inner jet suggests that they are part of the jet, which although undetected, remains collimated at these distances. The presence of optical emission at the knots, attributed to synchrotron emission by O'Dea et al. (1999) suggests the presence of shocks, considering the short lifetime (10–20 yr) of the optical synchrotron electrons.

2 OBSERVATIONS

2.1 1.6-GHz data reduction

The 1.6-GHz observation was made on 1998 July 4 (1998.52) using the 10-element Very Long Baseline Array (VLBA), the phased Very Large Array (VLA) and the VSOP orbiting antenna *HALCA* (only recording LCP) and is accompanied by a VLA observation made one day earlier, for the purpose of EVPA calibration.

The preliminary amplitude and phase calibration were done in the Astronomical Image Processing System (AIPS) using the standard techniques. The imaging was also carried out in the AIPS.

Due to the extended nature of the source (knots at $\sim$0.73 and $\sim$1.1 arcsec away from core), the self-calibration and imaging were done in four steps, starting with the inner VLBA (five antennas) and VLA, then adding BR, HN and NL, then MK and SC and finally, adding *HALCA*.

The instrumental polarizations (D-terms) for the ground antennas and *HALCA* were determined simultaneously with the polarization structure of 3C 380 using the AIPS task LPCAL. The continuous structure of 3C 380 makes it less than ideal for determining instrumental polarizations and to confirm the reliability of the results; the polarization calibration was repeated using only the ground antennas and the more-compact and unpolarized source, 3C 84. The instrumental polarizations of the ground antennas obtained by the two different runs were quite similar, leading us to believe that the *HALCA* instrumental polarization ($\sim$3 per cent) that was obtained using 3C 380 is reliable. The *HALCA* D-terms obtained here are also consistent with previous determinations of their values (Kembal et al. 2000).

Due to the $u-v$ plane asymmetry of the cross-hand polarization (*HALCA* has only LCP), the production of the linear polarization maps was done in the complex plane using the AIPS tasks CXPOLN and CXCLN.

2.2 5-GHz data reduction

The 5-GHz observations were made on 1998 April 9 using the 10-element VLBA. Calibration and imaging were performed in the standard way as described by Roberts, Wardle & Brown (1994) using the NRAO AIPS package. The instrumental polarization of each antenna was determined using a simple two-component model for the polarization of 3C 279.

We had no VLA data at this frequency. The UMRAO database (Aller et al. 1985) could not be used because of the large difference in RM between the two parsec-scale components of 3C 279 (Taylor 1998) and the 0.19-GHz difference in the frequency of the UMRAO and our observations. For this reason, we used the 1998 August 3 observation of 3C 279 by Taylor (2000) to perform the EVPA calibration. The reliability of the EVPA calibration is discussed in Section 2.3.

2.3 Uncertainties

The Faraday rotation images presented here were produced using two frequency observations separated by four months in time. In comparing the two images, it is assumed that the source structure has not changed in the four intervening months. The following evidence is cited in support of this assumption.

First, the expected motion of component A is less than 80 μas (Polatidis & Wilkinson 1998), much smaller than the beam size, and this (and similar motion across the source) should produce no discernible effects in the image. Secondly, where comparable, the derotated MVPAs that are deduced here (Section 3) compare well with those obtained by Taylor (1998). Significant changes may have occurred in the vicinity of the core and so comparison of the core properties (e.g. to obtain the spectrum) should be avoided.

2.3.1 EVPA calibration

The EVPA calibration for the 1.6-GHz observation was performed using VLA observations of the compact sources 1803+784 and 1732+389, which were also observed by the VLBA. The EVPA correction determined was then applied to the ground antennas + *HALCA* observation of 3C 380. The uncertainty in the 1.6-GHz EVPA has been estimated to be in the range of $\sim3^\circ$ to $\sim10^\circ$, with the uncertainty increasing from the polarization maximum towards the lowest polarization contour.

No integrated measurements were available for the EVPA calibration of the 5-GHz observations. As a result, it was necessary to use an indirect calibration procedure. The 5 GHz observations included scans of 3C 279, a quasar in which a component known as 'C4' (Taylor 2000), is often used for PA calibration. The closest observations available were those made in 1998 August 3 at 8 and 15 GHz reported by Taylor (2000). Using EVPA information and the RM at this epoch (-38 ± 50 rad m^{-2}), it was possible to calibrate the 5-GHz EVPA with an uncertainty in the range of $\sim8^\circ$ (at polarization maximum) to $\sim12^\circ$ (at lowest polarization contour). Strong evidence that no significant changes occurred to C4 in the months between Taylor's observations and those used here is provided by a 22-GHz monitoring of the knot by J.-L. Gomez (private communication). Five observations between 1998 March 9 and August 13 showed that the EVPA of C4 was constant to within two degrees during this time interval.

2.3.2 RM and MVPA accuracy

The Faraday rotation map has been created using only two frequencies (1.6 and 5 GHz), assuming that there is no aliasing in the RM for that region. This is a safe assumption since the previous measurements by Taylor (1998) report RM for the jet away from the core in the region of -30 ± 70 rad m^{-2}. Using the EVPA uncertainties in the 1.6-GHz VSOP and 5-GHz VLBA data from the current observation, it was possible to constrain the uncertainty in the RM and MVPA.

The need to use indirect methods to calibrate the 5-GHz EVPAs somewhat degraded our knowledge of the absolute position angles at 5 GHz, but not our ability to detect changes in position angle, since the same correction is applied to every pixel. Therefore, there are two uncertainties for the RMs and MVPAs. One describes the precision of the absolute values, while the other gives the precision with which spatial variations can be detected. The uncertainty in the absolute values depends on those in the corrected EVPAs at 1.6 GHz (3°) and at 5 GHz (8°). Using these values, the error in the absolute RM values is approximately 7 rad m^{-2}, while the error in absolute MVPA is 9°. However, taking the uncertainties in the uncorrected position angles at both frequencies to be about 3°, variations can be followed with an uncertainty of 2.5 rad m^{-2} in RM and 3.°5 in the MVPA.

3 DISCUSSION

3.1 Parsec-scale jet

Figs 1, 2 and 3 show total intensity contour maps of 3C 380 on three different scales. The figures also show the observed EVPA sticks not corrected for Faraday rotation.

The parsec-scale jet shows a continuous structure with a sharp bend at component A and apparent wiggles farther down the jet. The fractional polarization is relatively constant along the jet (∼10–20 per cent) with the exception that the fractional polarization increases to 30 per cent at the edges of the jet in the region between the knots A and E (Figs 4 and 5), behaviour also observed in the jets of 4C 71.07 (Hutchison, Cawthorne & Gabuzda 2001) as well as

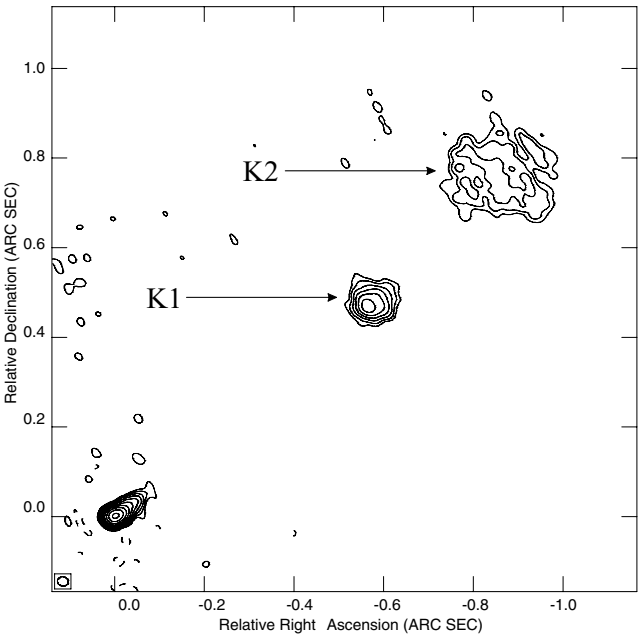

Figure 1. 1.6-GHz total intensity contours of 3C 380, produced using the inner VLBA (LA, OV, KP, PT, FD) and phased VLA. Peak flux density is 2.1 Jy beam^{-1}. First contour is 3.5 mJy beam^{-1}. Contour intervals at -1, 1, 2, 4 . . . times the first contour. The beam size is 24.0 × 20.7 mas.

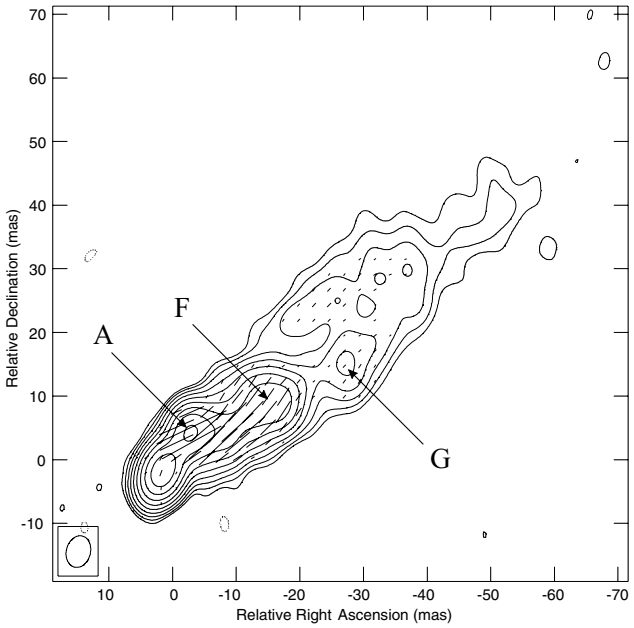

Figure 2. EVPA sticks (not corrected for Faraday rotation) superimposed on 1.6-GHz total intensity contours of 3C 380, produced using the VLBA and phased VLA. Peak flux density is 0.87 Jy beam^{-1}. First contour is 2 mJy beam^{-1}. Contour intervals at -1, 1, 2, 4 . . . times the first contour. Sticks of 1 mas length correspond to polarized flux density of 5.6 mJy beam^{-1}. The beam size is 5.0 × 3.7 mas.

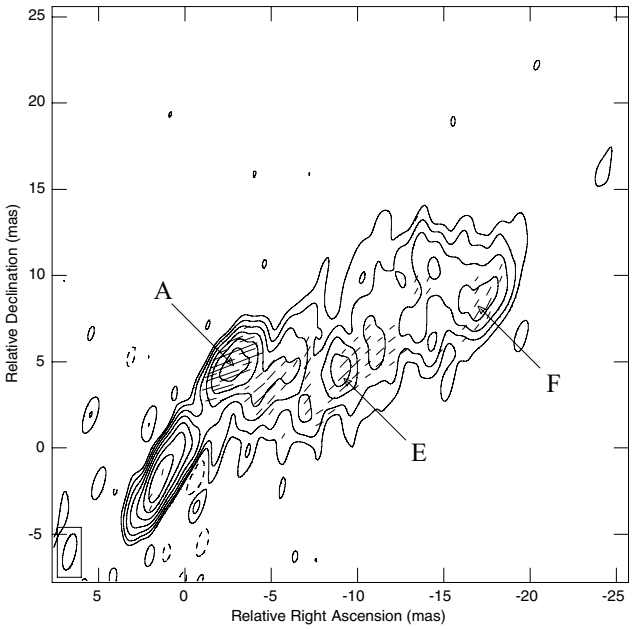

Figure 3. EVPA sticks (not corrected for Faraday rotation) superimposed on 1.6-GHz total intensity contours of 3C 380, produced using the VLBA, phased VLA and *HALCA*. Peak flux density is 47 mJy beam^{-1}. First contour is 4 mJy beam^{-1}. Contour intervals at -1, 1, 2, 4 . . . times the first contour. Sticks of 1 mas length correspond to polarized flux density of 12.5 mJy beam^{-1}. The beam size is 2.14 × 0.70 mas.

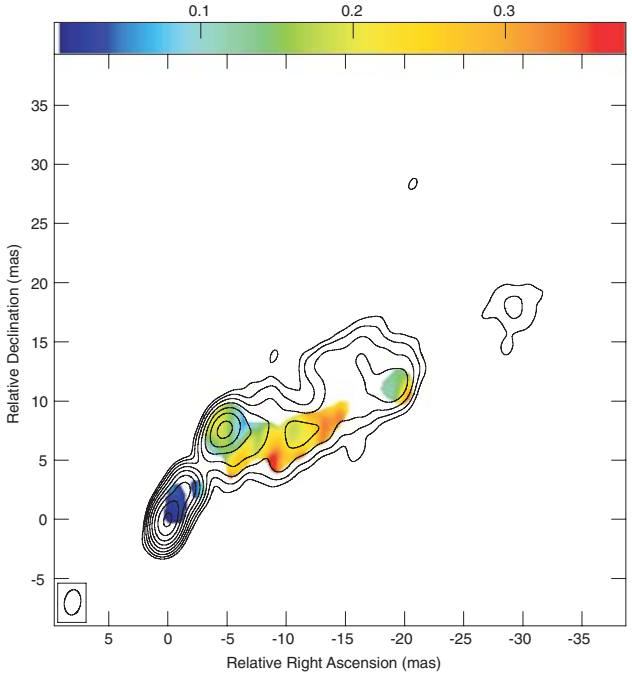

Figure 4. Fractional polarization map superimposed on 5-GHz total intensity contours of 3C 380. Peak flux density is 745 mJy beam^{-1}. First contour is 2.5 mJy beam^{-1}. Contour intervals at $-1, 1, 2, 4 \ldots$ times the first contour. The beam size is 2.14 × 1.37 mas.

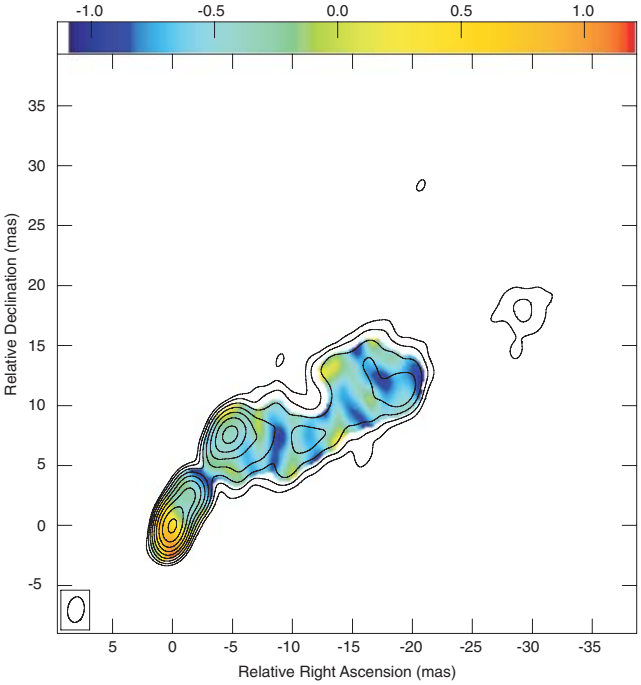

Figure 6. Spectral index map (1.6–5 GHz) superimposed on 5-GHz total intensity contours of 3C 380. Peak flux density is 745 mJy beam^{-1}. First contour is 2.5 mJy beam^{-1}. Contour intervals at -1, 1, 2, 4 ... times the first contour. The beam size is 2.14 × 1.37 mas.

Mrk 501 (Pushkarev et al. 2005) and 1055+018 (Attridge, Roberts & Wardle 1999). The increase in fractional polarization could be attributed to a more organized magnetic field at the region, an effect which could be the result of compression due to interaction with an external medium. Another possibility is that this polarization edge-brightening is due to the geometry of the magnetic field, an effect predicted by models of magnetic fields with a helical geometry (Laing 1981). Asada et al. (2002) and Gabuzda, Murray & Cronin (2004) have reported RM distributions consistent with such magnetic field geometries.

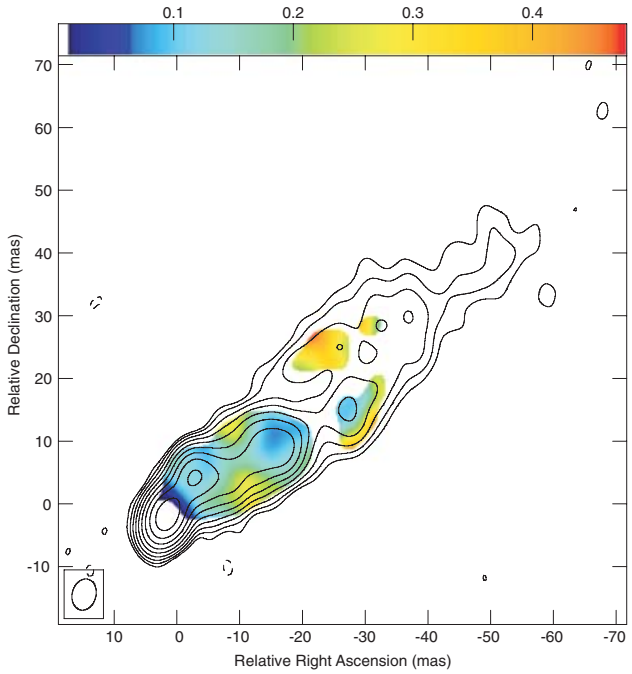

Figure 5. Fractional polarization map superimposed on 1.6-GHz total intensity contours of 3C 380. Peak flux density is 874 mJy beam^{-1}. First contour is 2 mJy beam^{-1}. Contour intervals at $-1, 1, 2, 4 \ldots$ times the first contour. The beam size is 5.0 × 3.7 mas.

The spectral index distribution (Figs 6 and 7) reveals the parsec-scale jet to be optically thin, with $\alpha \sim -0.7$. It has been reported by Kameno et al. (2000b) that there are regions in the jet where the spectral index becomes positive, attributed to adiabatic expansion of plasma blobs. These inversions are present in the spectral index maps made as part of this study, but their significance seems marginal in view of the large uncertainties (∼0.5–1.0) in the spectral index measurement in regions of low flux density. It is possible that they may arise from non-uniform $u-v$ coverage and/or the difference in the $u-v$ coverage between the two frequencies.

The RM (Figs 8 and 9) is quite small, ranging from -30 to -45 rad m^{-2}, in agreement with previous reports (Taylor 1998). Considering the uncertainty of ∼2.6 rad m^{-2}, the small-scale RM map (Fig. 8) reveals significant evidence of variation, with the RM abruptly increasing by 10 rad m^{-2} (from -35 to -45 rad m^{-2}) just west of component A, beyond which it gradually decreases again. Such a large gradient in RM (assuming that it is due to external Faraday rotation) seems to rule out a large-scale Faraday screen that is distant from the source and is more consistent with variations in the gas density and/or magnetic fields of ionized material in the vicinity of the jet, well outside the nuclear region.

Using the RM information, it was possible to produce images of the MVPA distribution (Figs 8 and 9). The images reveal an abrupt rotation in the MVPAs (by ∼45°) immediately downstream of component A, beyond which point the MVPAs are relatively constant.

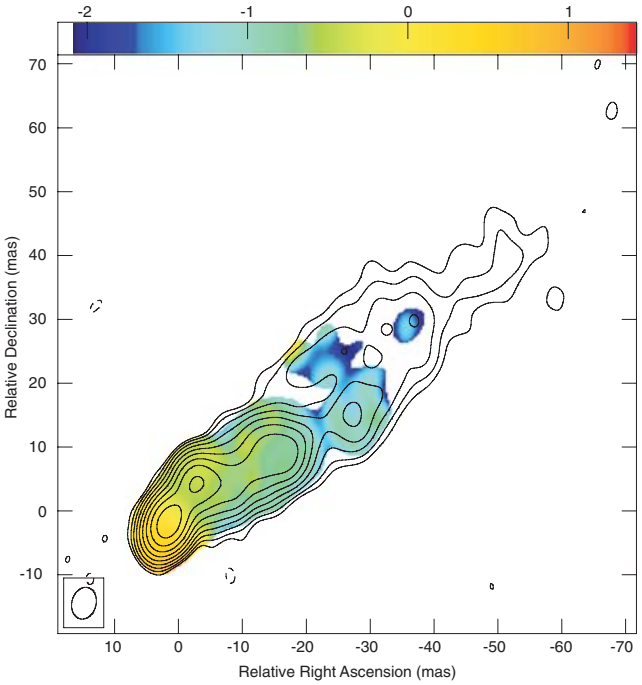

Figure 7. Spectral index map (1.6–5 GHz) superimposed on 1.6-GHz total intensity contours of 3C 380. Peak flux density is 874 mJy beam^{-1}. First contour is 2 mJy beam^{-1}. Contour intervals at $-1, 1, 2, 4 \ldots$ times the first contour. The beam size is 5.0 × 3.7 mas.

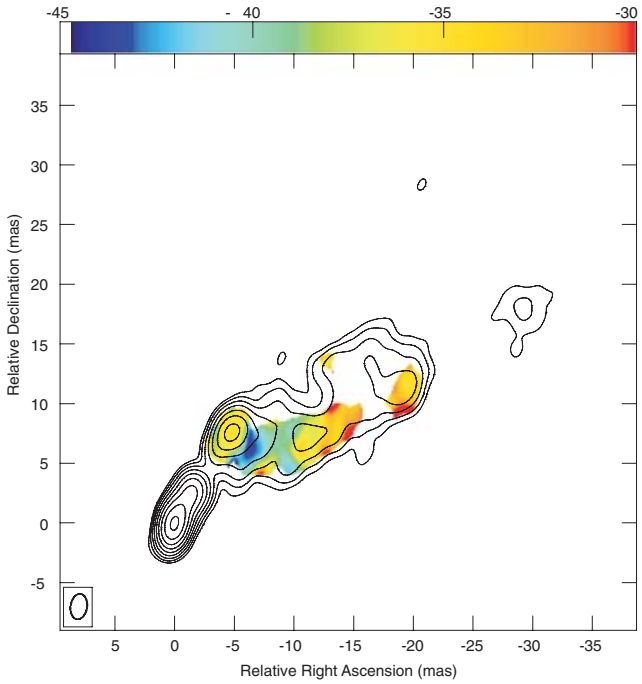

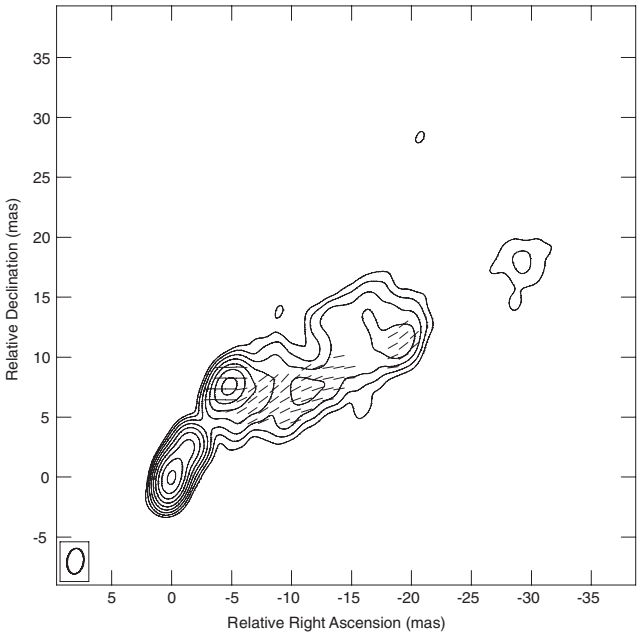

Figure 8. Top panel: RM map superimposed on 5-GHz total intensity contours of 3C 380. Bottom panel: MVPA sticks of constant length superimposed on 5-GHz total intensity contours of 3C 380. Absence of RM values and subsequently the MVPAs at the core is due to lack of 1.6-GHz polarization there. Peak flux density is 745 mJy beam^{-1}. First contour is 2 mJy beam^{-1}. Contour intervals at $-1, 1, 2, 4 \ldots$ times the first contour. The beam size in both images is 2.14 × 1.37 mas.

3.2 Component A

3.2.1 Current and past observations

(i) *Kinematics*. The motion of component A has been monitored for the past two decades and it has been shown to move superluminally (Polatidis & Wilkinson 1998). The most recent published value of its velocity is $\beta_{\rm app} = 6.86 \pm 0.17$ with a proper motion of $\mu = 0.235 \pm 0.006$ mas yr^{-1}, based on 5-GHz VSOP data (Kameno et al. 2000a). Fig. 10 shows a plot of distance from the core against time; the values used are presented in Table 1.

(ii) *Polarization*. The polarization properties of component A have been studied by Cawthorne et al. (1993) and Taylor (1998). Cawthorne reported fractional polarization of 4 per cent at 5 GHz, whereas Taylor reported a fractional polarization of 12 per cent for his 4.6–5.1 GHz data. Both the 5- and 1.6-GHz images from the current observation show fractional polarization ranging from 8 to 20 per cent. When convolved with a beam comparable to those used for the earlier observations, component A has fractional polarization value of 14.9 ± 2.6 per cent. When plotted against time, the fractional polarization appears to be increasing (Fig. 11).

Component A shows structure in the fractional polarization distribution in both the 1.6- and 5-GHz images. This suggests that the structure is not an artefact of the $u-v$ coverage and is likely to be real. The fractional polarization peaks at a value ∼20 ± 5 per cent at the north-eastern edge of the knot and there is a deep minimum of ∼8 ± 1 per cent on the western side. The ridge line of the jet continues to the west, and beyond the knot, the fractional polarization again increases to ∼8 per cent. The dip in polarization is almost certainly due to cancellation, since it occurs in a region where there is a large gradient in the EVPA.

(iii) *Faraday rotation and MVPA*. At component A, the RM has a value of -35 ± 4 rad m^{-2} (Table 2),which is in agreement with (though much more precise than) the value of 4 ± 50 rad m^{-2} reported by Taylor (1998).

The Faraday-corrected EVPA at component A implies an MVPA with an orientation of $-91^\circ \pm 9^\circ$, which is neither perpendicular nor parallel to the proper motion angle ($-31^\circ \pm 2^\circ$) of the component (Kameno et al. 2000a). Taylor (1998) reported an MVPA for the component of -84° with an uncertainty of 4° [The uncertainty is

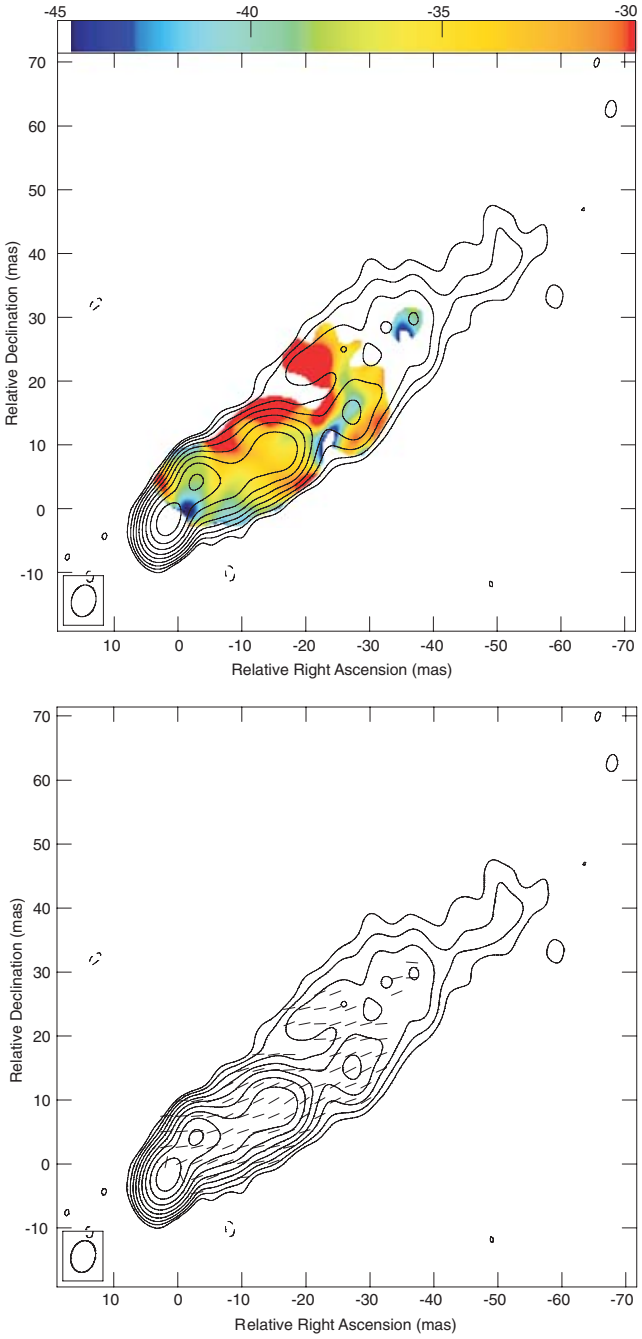

Figure 9. Top panel: RM map superimposed on 1.6-GHz total intensity contours of 3C 380. Bottom panel: MVPA sticks of constant length superimposed on 1.6-GHz total intensity contours of 3C 380. Although polarization is present in both 1.6- and 5-GHz cores, RM values and subsequently the MVPAs have been blanked there. Peak flux density is 874 mJy beam^{-1}. First contour is 2 mJy beam^{-1}. Contour intervals at -1, 1, 2, 4 . . . times the first contour. The beam size in both images is 5.0 × 3.7 mas.

estimated here based on the uncertainties on EVPA and RM mentioned by Taylor (1998).]

3.3 Knot K1

Although the jet of 3C 380 is visible only up to ∼70 mas, two knots of emission (K1 and K2) appear at distances ∼0.73 and ∼1 arcsec

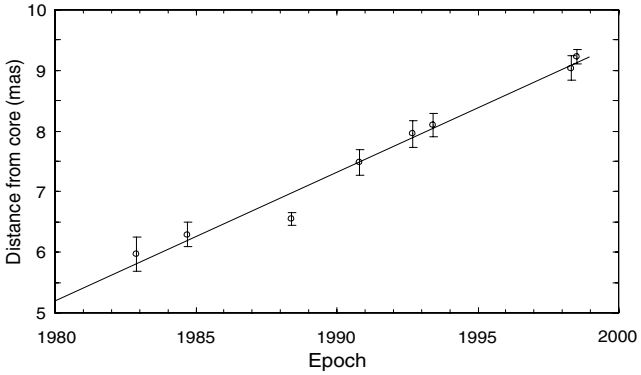

Figure 10. Distance of component A from the 5-GHz core plotted against time.

Table 1. Distance and position angle of component A relative to the core at 5 GHz.

Epoch	Distance (mas)	Position angle (°)	Reference
1982.9	5.97 ± 0.28	−30.9	1
1984.7	6.29 ± 0.20	−31.0	1
1988.4	6.55 ± 0.10	−28.5	1
1990.8	7.48 ± 0.21	−29.9	1
1992.7	7.95 ± 0.22	−30.0	1
1993.4	8.10 ± 0.20	−30.4	1
1998.3	9.04 ± 0.20	−32.0	2
1998.5	9.22 ± 0.05	−31.2	3

References. (1) Polatidis & Wilkinson (1998). (2) This work. (3) Kameno et al. (2000a).

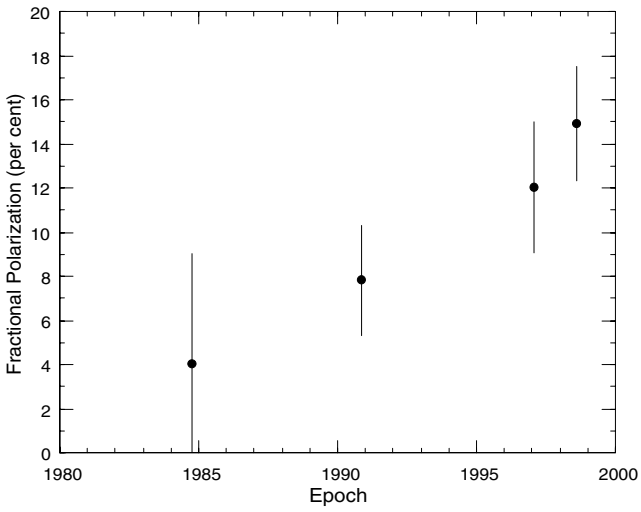

Figure 11. 5-GHz fractional polarization of component A against time.

north-west from the core (Fig. 1). Previous observations of the knots show emission not only in the radio but also in the optical (De Vries et al. 1997; O'Dea et al. 1999). The good one-to-one correspondence between the radio and optical emission at the knots suggests that the optical emission is most likely synchrotron emission. Due to the short lifetime of the optical synchrotron electrons (10–20 yr), the presence of the optical knots requires re-acceleration within these regions, most likely associated with shocks. Our observations show

Table 2. 5-GHz fractional polarization (m), RM and MVPA (θ_B) of component A at different epochs.

Epoch	m	σ_m	RM	$\sigma_{\rm RM}$	θ_B	σ_{θ_B}	Reference
1984.8	4.0	6.0[a]	–	–	–	–	1
1990.9	7.8	2.5	–	–	–	–	2
1997.1	12.0	3.0[a]	4	50	−84	4.3[b]	3
1998.3	14.9	2.6	−35	4	−91	7.0	4

References. (1) Cawthorne et al. (1993). (2) Cawthorne unpublished. (3) Taylor (1998). (4) This work.
Notes. [a]Error estimated from published image, using I and P lowest contour and I and P peak flux density of component A. [b]Error estimated from EVPA and RM uncertainties of 2° and 70 rad m^{-2}, respectively, as mentioned by Taylor (1998).

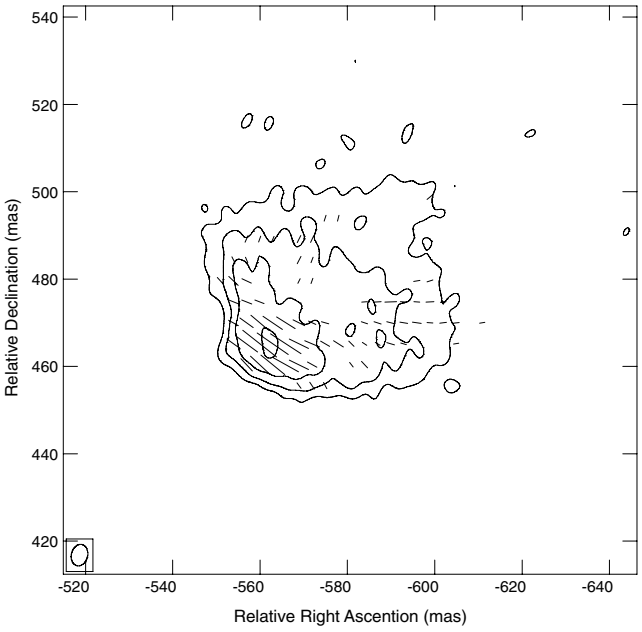

Figure 12. Faraday derotated MVPA sticks superimposed on 1.6-GHz total intensity contours of knot K1 in 3C 380. Peak flux density is 148 mJy beam^{-1}. First contour is 2 mJy beam^{-1}. Contour intervals at $-1, 1, 2, 4 \ldots$ times the first contour. The beam size is 5.0 × 3.7 mas.

the knot K1 both in total and polarized intensities at the highest resolution published so far, revealing an unusual structure (Fig. 12). The total intensity image shows a structure that could be described as an inverted bow shock, with the intensity peaking in the direction towards the core and fading away in the opposite direction. The knot is also polarized, with fractional polarization peaking at ∼40 per cent of the total intensity maximum.

The MVPA distribution at the knot appears tangential to the bow ridge in the south-eastern part of the knot while fanning away radially in the north-western part. For the determination of the MVPA, the EVPAs have been corrected for an RM of −45 rad m^{-2}, derived from the 1.6- and 5-GHz polarization images. Since no previous RM observations of K1 exist, it is unknown whether there is any 180° ambiguity; it is assumed here that the RM is quite small and therefore no such ambiguity exists. The RM value presented here is the smallest given by the observed polarization angles at 1.6 and 5 GHz.

The structures in total intensity and polarization are reminiscent of those expected for a conical shock wave, such as arises when

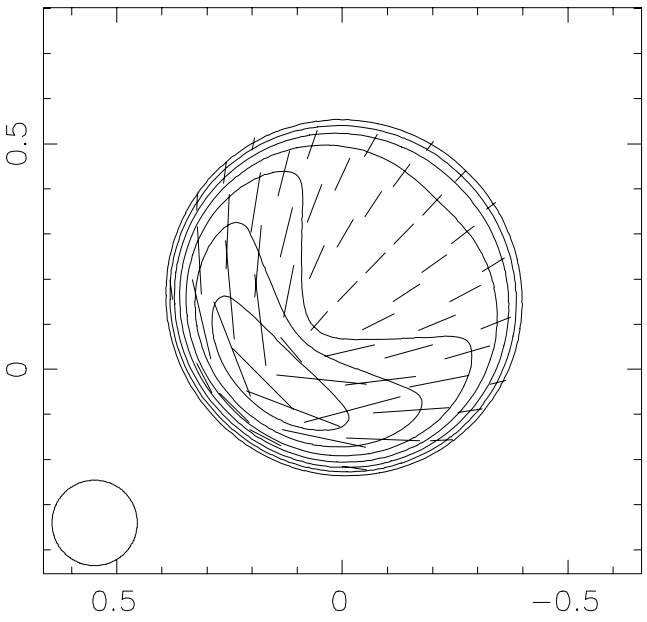

Figure 13. MVPA sticks superimposed on total intensity contours as predicted by the conical shock model. Model parameters: angle to the line of sight at shock frame $\theta = 10°$, cone half-angle $\eta = 20°$, fraction of magnetic field in tangled form $f = 0.5$, and upstream plasma velocity at shock frame $\beta_{\rm u} = 0.95$.

the jet becomes temporarily overpressured (Bowman, Leahy & Komissarov 1996; Agudo et al. 2001). A simple model for such structures has been presented (Cawthorne & Cobb 1990; Cawthorne 2006), where the shock is modelled as a conical discontinuity with emission arising only near the surface. For comparison, a simulation is presented for a cone half-opening angle of 20°, viewing angle (between the axis and line of sight) of 10° and an upstream magnetic field structure where 50 per cent of the energy is in a component parallel to the flow and 50 per cent is in a disordered field (Fig. 13; see Cawthorne 2006 for more details). The upstream flow velocity $\beta_{\rm u} = 0.95$. The contours are of total intensity and MVPA sticks are plotted. The model has been convolved with beam plotted in the lower left-hand panel of the figure. The figure has been rotated so that the axis in the model and the jet direction inferred for 3C 380 are approximately parallel.

The image and model share the following features. The total intensity contours peak at the leading edge of the structure. In this region, the MVPAs are perpendicular to the jet direction, while downstream, they fan radially away from the peak intensity. The peak fractional polarization in the image is about 40 per cent, while that predicted by the model is ∼30 per cent. Here, the intention is not to suggest a detailed model for the component, but merely to demonstrate that conical shock waves can produce structures similar to that observed for the knot K1 in the jet of 3C 380.

4 CONCLUSIONS

This work presents the results from two single-frequency observations of 3C 380 using data obtained with the VSOP at 1.6 GHz and the VLBA at 5 GHz. This combination of instruments and frequencies provides a means to study multifrequency properties of parsec-scale jets on scales not probed by ground-based VLBI, as is demonstrated by the following findings.

(i) The observations have made it possible to study small variations in the RM ($\leqslant$10 rad m^{-2}) at the highest angular resolution to date. Variations in the RMs and MVPAs were obtained on scales of a few mas with uncertainties of 2.6 rad m^{-2} and 3.°4, respectively. The uncertainties in the absolute values of the RM and MVPA were considerably poorer, due to the indirect method used to calibrate the 5-GHz polarization angles.

(ii) The high-resolution RM map obtained using the space baselines revealed significant variations in the RM previously unseen from ground-based observations. In particular, the RM increases abruptly in the region just west of component A, suggesting the presence of an external ionized cloud in the vicinity of the jet.

(iii) The fractional polarization of the bright feature, component A, where the jet bends, has increased to 15 per cent. A comparison with previous observations shows that the fractional polarization has increased steadily from 4 to 15 per cent over 15 yr. The RM of component A is -35 ± 4 rad m^{-2}, a more precise estimate than that which was obtained previously. The MVPA is $-91^\circ \pm 9^\circ$, at an oblique angle to both the component motion and the apparent ridge line of the jet.

(iv) The distant knots K1 and K2 have been imaged at the highest resolution to date and the first maps of their polarization properties obtained. Our multifrequency observation enabled us to map the Faraday derotated MVPA distribution at knot K1. The total intensity map reveals a structure that can be described as an inverted bow shock with total intensity peaking towards the direction of the core and fading away in the opposite direction. The MVPA distribution reveals the projected magnetic field to be tangential to the bow ridge while fanning radially outwards in the opposite direction. This structure shows remarkable qualitative similarities to predictions made by conical shock models.

ACKNOWLEDGMENTS

AP acknowledges the following. University of Central Lancashire for the PhD funding (during which the work presented in this paper was performed). JIVE, the Netherlands, for providing accommodation, facilities and expertise for two weeks, during the analysis of the data. The European Community's Human Potential Programme under contract HPRN-CT-2002-00321 for currently funding a postdoctoral position (under the ENIGMA Research Training Network). TVC acknowledges the support of PPARC research grants. The authors thank the referee for useful comments and acknowledge the use of the *HALCA* satellite, which is provided by the Japanese Institute of Space and Astronautical Science via the VSOP project, in cooperation with many organizations and radio telescopes around the world. The VLBA, VLA and AIPS image-processing software are facilities provided and maintained by the National Radio Astronomy Observatory, which is a facility of the National Science Foundation operated under cooperative agreement by Associated Universities, Inc.

REFERENCES

Agudo I., Gómez J.-L., Martí J.-M., Ibáñez J.-M., Marscher A. P., Alberdi A., Aloy M.-A., Hardee P. E., 2001, ApJ, 549, 183
Aller H. D., Aller M. F., Latimer G. E., Hodge P. E., 1985, ApJS, 59, 513
Asada K., Inoue M., Uchida Y., Kameno S., Fujisawa K., Iguchi S., Mutoh M., 2002, PASJ, 54, 39
Attridge J. M., Roberts D. H., Wardle J. F. C., 1999, ApJ, 518, 87
Bowman M., Leahy J. P., Komissarov S. S., 1996, MNRAS, 279, 899
Cawthorne T. V., 2006, MNRAS, 367, 851
Cawthorne T. V., Cobb W. K., 1990, ApJ, 350, 536
Cawthorne T. V., Wardle J. F. C., Roberts D. H., Gabuzda D. C., Brown L. F., 1993, ApJ, 416, 496
de Vries W. H. et al., 1997, ApJS, 110, 191
Gabuzda D. C., Murray É., Cronin P., 2004, MNRAS, 351, 89
Hutchison J. M., Cawthorne T. V., Gabuzda D. C., 2001, MNRAS, 321, 525
Kameno S., Inoue M., Fujisawa K., Shen Z.-Q., Wajima K., 2000a, PASJ, 52, 1045
Kameno S., Shen Z.-Q., Inoue M., Fujisawa K., Wajima K., 2000b, in Hirabayashi H., Edwards P. G., Murphy D. W., eds, Proc. VSOP Symp., Astrophysical Phenomena Revealed by Space VLBI. Inst. Space Astronautical Sci., Sagimahara, p. 63
Kemball A. et al., 2000, PASJ, 52, 1055
Laing R. A., 1981, ApJ, 248, 87
O'Dea C. P., de Vries W., Biretta J. A., Baum S. A., 1999, ApJ, 117, 1143
Polatidis A., Wilkinson P. N., 1998, MNRAS, 294, 327
Pushkarev A. B., Gabuzda D. C., Vetukhnovskaya Yu. N., Yakimov V. E., 2005, MNRAS, 356, 859
Roberts D. H., Wardle J. F. C., Brown L. F., 1994, ApJ, 427, 718
Taylor G. B., 1998, ApJ, 506, 637
Taylor G. B., 2000, ApJ, 533, 95
Wilkinson P. N., Akujor C. E., Cornwell T. J., Saikia D. J., 1991, MNRAS, 248, 86

This paper has been typeset from a TEX/LATEX file prepared by the author.